

Competition between electric field and magnetic field noise in the decoherence of a single spin in diamond

P. Jamonneau,¹ M. Lesik,¹ J. P. Tetienne,¹ I. Alvizu,² L. Mayer,¹ A. Dréau,¹ S. Kosen,¹ J.-F. Roch,¹ S. Pezzagna,³ J. Meijer,³ T. Teraji,⁴ Y. Kubo,⁵ P. Bertet,⁵ J. R. Maze,² and V. Jacques^{1,6,*}

¹Laboratoire Aimé Cotton, CNRS, Université Paris-Sud, ENS Cachan, Université Paris-Saclay, 91405 Orsay Cedex, France

²Facultad de Física, Pontificia Universidad Católica de Chile, Santiago 7820436, Chile

³Department of Nuclear Solid State Physics, Institute for Experimental Physics II, Universität Leipzig, Linnzstrasse 5, 04103 Leipzig, Germany

⁴National Institute for Materials Science, 1-1 Namiki, Tsukuba, Ibaraki 305-0044, Japan

⁵Quantronics group, SPEC, CEA, CNRS, Université Paris-Saclay, CEA Saclay 91191 Gif-sur-Yvette, France

⁶Laboratoire Charles Coulomb, Université de Montpellier and CNRS, 34095 Montpellier, France

(Received 25 November 2015; published 25 January 2016; corrected 6 June 2019)

We analyze the impact of electric field and magnetic field fluctuations in the decoherence of the electronic spin associated with a single nitrogen-vacancy (NV) defect in diamond. To this end, we tune the amplitude of a magnetic field in order to engineer spin eigenstates protected either against magnetic noise or against electric noise. The competition between these noise sources is analyzed quantitatively by changing their relative strength through modifications of the host diamond material. This study provides significant insights into the decoherence of the NV electronic spin, which is valuable for quantum metrology and sensing applications.

DOI: [10.1103/PhysRevB.93.024305](https://doi.org/10.1103/PhysRevB.93.024305)

Improving the coherence time of solid-state spin qubits is a central challenge in quantum technologies. Decoherence is induced by fluctuations of the local environment and can be mitigated by following several strategies. On one hand, the tools of material science can be exploited to engineer host samples with quantum grade purity [1]. As an example, millisecond-long coherence times have been achieved for electron spin impurities in isotopically purified diamond samples at room temperature [1,2], while a few seconds can be obtained in purified silicon at low temperature [3]. On the other hand, the coherence time can be improved through active quantum control of the many-body environment [4–7] or by decoupling the central spin from its fluctuations, either by applying periodic spin flips [8–10] or by engineering spin eigenstates which are protected against environmental noise [11–14]. However, for these strategies to be effective, it is crucial to first identify the sources of noise and understand precisely their impact on the coherence properties of the central spin.

Here, we analyze how magnetic and electric field fluctuations impair the quantum coherence of the electronic spin associated with a single nitrogen-vacancy (NV) defect in diamond. This atomic-sized defect is attracting considerable interest for a broad range of applications, including quantum metrology and sensing [15–17], quantum information processing [18], and hybrid quantum systems [19–21]. For all these applications, optimal performances require a long spin coherence time. In this paper, we analyze the contributions of magnetic and electric field fluctuations to spin decoherence by exploiting spin eigenstates protected either against magnetic noise or against electric noise [22]. The competition between these noise sources is then analyzed quantitatively by changing their relative strength through modifications of the NV defect environment.

The NV defect in diamond has a spin triplet ground state $S = 1$ with a zero-field splitting $D \approx 2.88$ GHz between the $m_s = 0$ and $m_s = \pm 1$ spin sublevels, where m_s denotes the spin projection along the NV symmetry axis (z). The spin Hamiltonian describing the ground state in the presence of strain, electric field \mathbf{E} , and magnetic field \mathbf{B} has been discussed in detail in Refs. [22,23]. The strain, which is induced by a local deformation of the diamond crystal, can be treated as a local static electric field $\boldsymbol{\Sigma}$ interacting with the NV defect through the linear Stark effect [24]. Defining a total effective electric field $\boldsymbol{\Pi} = \boldsymbol{\Sigma} + \mathbf{E}$, the spin Hamiltonian can be written as

$$H = (hD + d_{\parallel}\Pi_z)S_z^2 + g_e\mu_B\mathbf{S} \cdot \mathbf{B} - d_{\perp}[\Pi_x(S_xS_y + S_yS_x) + \Pi_y(S_x^2 - S_y^2)], \quad (1)$$

where $\mathbf{S} = \{S_x, S_y, S_z\}$ are the dimensionless electron spin operators, h is the Planck constant, $d_{\parallel}/h = 0.35$ Hz cm V⁻¹ and $d_{\perp}/h = 17$ Hz cm V⁻¹ are the longitudinal and transverse components of the electric dipole moment [25], g_e is the electron g factor, and μ_B is the Bohr magneton. For weak magnetic fields such that $B \ll hD/g_e\mu_B$, the transverse components of the Zeeman interaction can be neglected and the eigenstates of the spin system are $\{|0\rangle, |+\rangle, |-\rangle\}$, where

$$|+\rangle = \cos\left(\frac{\theta}{2}\right)|+1\rangle + \sin\left(\frac{\theta}{2}\right)e^{i\phi}|-1\rangle, \\ |-\rangle = \sin\left(\frac{\theta}{2}\right)|+1\rangle - \cos\left(\frac{\theta}{2}\right)e^{i\phi}|-1\rangle.$$

Here, $\{|m_s\rangle\}$ are the eigenstates of the S_z operator, $\tan\phi = \Pi_y/\Pi_x$ and

$$\tan\theta = \frac{\xi_{\perp}}{\beta_z},$$

where $\xi_{\perp} = d_{\perp}\sqrt{\Pi_x^2 + \Pi_y^2}/h$ and $\beta_z = g_e\mu_B B_z/h$.

*vincent.jacques@umontpellier.fr

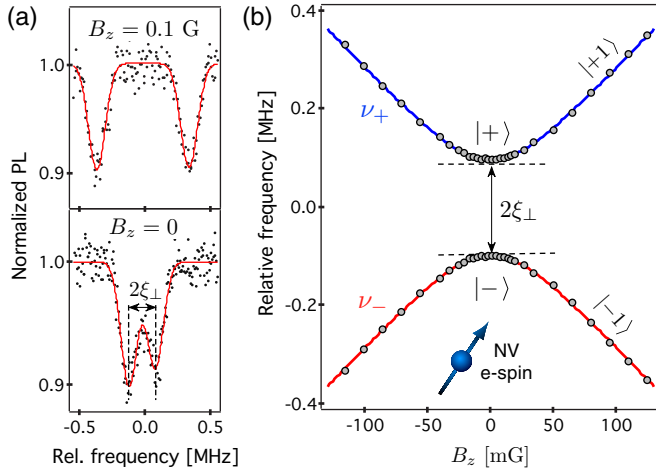


FIG. 1. (a) Typical ESR spectra recorded from a single NV defect hosted in a high-purity diamond crystal around $B_z = 0$. The ESR transitions are associated with the ^{14}N nuclear spin projection $m_I = 0$. Those linked to $m_I = \pm 1$ are not shown. (b) ESR frequencies ν_+ and ν_- as a function of B_z . The solid lines are data fitting with Eq. (2), leading to $\xi_\perp = 93 \pm 2$ kHz.

Since $d_\parallel \ll d_\perp$ [25,26], we neglect the longitudinal component of the Stark effect and the frequencies ν_\pm of the electron spin resonance (ESR) transitions $|0\rangle \rightarrow |\pm\rangle$ are given by

$$\nu_\pm = D \pm \sqrt{\xi_\perp^2 + \beta_z^2}. \quad (2)$$

In bulk diamond samples ξ_\perp is in the range of 100 kHz (Fig. 1) and can reach a few MHz for NV defects hosted in nanodiamonds, where the intrinsic strain is much stronger [27].

In the limit $\beta_z \gg \xi_\perp$, i.e., for $\theta \approx 0$, the eigenstates are those of the S_z operator and the ESR frequencies evolve linearly with the axial magnetic field [see Fig. 1(b)]. In this regime, decoherence of the NV defect electron spin is usually dominated by magnetic field noise. On the other hand, if $\beta_z \ll \xi_\perp$, i.e., for $\theta \approx \pi/2$, the ESR frequencies are given by $\nu_\pm = D \pm \xi_\perp$ and the NV defect electron spin is protected against first-order magnetic field fluctuations since $\langle \pm | S_z | \pm \rangle = 0$. Decoherence is then dominated by strain/electric field noise and second-order (quadratic) magnetic field fluctuations. In the following, we analyze the impact of these fluctuations on the spin coherence by tuning the strength of B_z . In most of the diamond samples, an enhancement of the coherence time is expected at zero magnetic field, as previously reported in Ref. [22].

Individual NV defects are optically isolated at room temperature using a scanning confocal microscope under green laser excitation. A coil is used to precisely control the magnetic field amplitude B_z along the NV axis and ESR transitions are driven with a microwave field applied through a copper microwire spanned on the diamond surface. The nitrogen atom of the defect is a ^{14}N isotope (99.6% abundance), corresponding to a nuclear spin $I = 1$. Each electron spin state is therefore split into three hyperfine sublevels. In the following, we focus on electron spin transitions associated with the ^{14}N nuclear spin projection $m_I = 0$, so that the spin Hamiltonian (1) is not modified by the hyperfine interaction [26]. ESR spectra recorded from a single NV defect around zero magnetic field

are shown in Fig. 1(a). The ESR frequencies closely follow Eq. (2) with an anticrossing at $B_z = 0$, where $\nu_+ - \nu_- = 2\xi_\perp$ [Fig. 1(b)].

We first consider *native* NV defects hosted in an isotopically purified diamond crystal ($^{13}\text{C} = 0.002\%$) grown by chemical vapor deposition (CVD) [28]. Decoherence of the NV defect electron spin is analyzed through measurements of the free-induction decay (FID) while applying the usual Ramsey sequence $(\pi/2) - \tau - (\pi/2)$ [29]. Typical FID signals recorded at different magnetic field amplitudes B_z are shown in Fig. 2(a). Surprisingly, a pronounced *dip* of the coherence time T_2^* is observed around zero magnetic field [Fig. 2(c)].

To understand this behavior, we introduce the random variables $\delta\beta_z$ and $\delta\xi_\perp$, which describe the temporal fluctuations of the magnetic and electric fields around their mean values β_z and ξ_\perp . In the limit $\beta_z \gg \xi_\perp$, the coherence time is given by $T_{2,\beta_z \gg \xi_\perp}^* = 1/\sqrt{2\pi\sigma_{\beta_z}}$, where $\sigma_{\beta_z}^2 = \langle \delta\beta_z^2 \rangle$ is the variance of the magnetic field fluctuations [26]. In this regime, decoherence is governed by magnetic noise. When the spin system is approaching the level anticrossing, the fluctuation of the ESR frequency $\delta\nu$ can be expressed as

$$\delta\nu = \delta\xi_\perp \sin\theta + \delta\beta_z \cos\theta,$$

leading to a decay of the FID signal with a coherence time [26]

$$T_2^* = \frac{1}{\sqrt{2\pi\sigma_{\xi_\perp}}} \sqrt{\frac{1 + \left(\frac{\beta_z}{\xi_\perp}\right)^2}{1 + \left(\frac{\beta_z}{\xi_\perp}\right)^2 \left(\frac{\sigma_{\beta_z}}{\sigma_{\xi_\perp}}\right)^2}}. \quad (3)$$

Here, $\sigma_{\xi_\perp}^2 = \langle \delta\xi_\perp^2 \rangle$ is the variance of the electric field fluctuations. We stress that such a simple analytic formula is valid (i) if $(\sigma_{\beta_z}, \sigma_{\xi_\perp}) \ll \xi_\perp$ and (ii) if the second-order magnetic field fluctuations of the ESR frequency can be neglected, i.e., for $\sigma_{\beta_z}^2/2\xi_\perp \ll \sigma_{\xi_\perp}$ [26].

At the level anticrossing $T_{2,\beta_z=0}^* = 1/\sqrt{2\pi\sigma_{\xi_\perp}}$, which indicates that the coherence time is limited by electric noise. In order to analyze the behavior of T_2^* around the anticrossing, we introduce the parameter

$$\mathcal{R} = \frac{T_{2,\beta_z=0}^*}{T_{2,\beta_z \gg \xi_\perp}^*} = \frac{\sigma_{\beta_z}}{\sigma_{\xi_\perp}}. \quad (4)$$

If $\sigma_{\beta_z} < \sigma_{\xi_\perp}$, the coherence time drops around zero field ($\mathcal{R} < 1$), as experimentally observed in Fig. 2(c) for a single NV defect hosted in an isotopically purified diamond sample. Data fitting with Eq. (3) leads to $\sigma_{\beta_z} = 2.20 \pm 0.06$ kHz and $\sigma_{\xi_\perp} = 8.0 \pm 0.2$ kHz, corresponding to $\mathcal{R} = 0.28 \pm 0.05$. This result reveals the existence of a significant source of electric field noise. It is known that a two-photon ionization process of the NV defect can promote charge carriers to the conduction band of diamond [30–32]. This mechanism was recently used to demonstrate photoelectric detection of the electron spin resonance [33]. Here, charge fluctuations induced by photoionization of the NV defect produce an electric field noise, which is likely the dominant decoherence mechanism in zero magnetic field. This source of electric noise is intrinsically linked to the optical illumination of the NV defect, which is required for polarization and readout of its electronic spin. For deep native NV defects in isotopically purified diamond

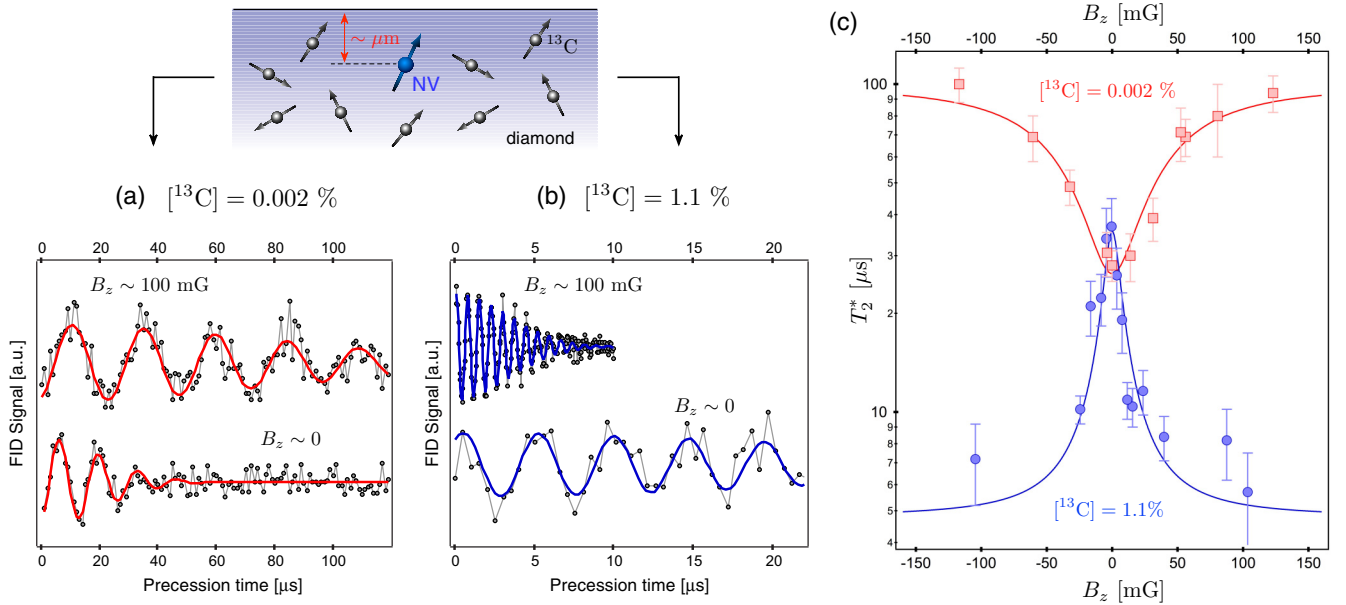


FIG. 2. (a), (b) Typical FID signals recorded at $B_z = 0.1$ G (top) and $B_z \sim 0$ (bottom) from a native single NV defect hosted in a high-purity diamond sample with (a) $[^{13}\text{C}] = 0.002\%$ and (b) $[^{13}\text{C}] = 1.1\%$. In both cases, the NV defects are lying few micrometers below the diamond surface and $\xi_{\perp} \sim 100$ kHz. The coherence time T_2^* is extracted by fitting the FID signal with the function $\cos(2\pi\Delta\tau) \exp[-(\tau/T_2^*)^2]$, where Δ is the detuning between the microwave excitation and the ESR frequency. In (a), it was checked that no revivals could be observed for a longer precession time. (c) Evolution of T_2^* (log scale) as a function of B_z in the two samples with different contents of ^{13}C isotopes. The red solid line is data fitting with Eq. (3). The blue solid line is a Lorentzian fit used as a guide to the eye.

samples, applying a static magnetic field enables one to protect the central spin against this intrinsic source of electric noise.

If $\sigma_{\beta_z} > \sigma_{\xi_{\perp}}$, the coherence time is expected to increase at the level anticrossing. This regime can be reached by increasing σ_{β_z} . In high-purity diamond samples, the magnetic noise originates from the fluctuations of a bath of ^{13}C nuclear spins ($I = 1/2$). Increasing the amplitude of these fluctuations can be simply achieved by increasing the ^{13}C content during the CVD growth [1,2]. Typical FID signals recorded around zero field for a single NV defect hosted in a commercial CVD-grown diamond sample with a natural content of ^{13}C isotopes (1.1%) are shown in Fig. 2(b). The evolution of T_2^* with B_z now reveals a coherence peak at zero magnetic field [Fig. 2(c)], as reported in Ref. [22]. This observation indicates that magnetic noise is now the strongest source of decoherence. In the limit $\beta_z \gg \xi_{\perp}$, we measure $T_{2,\beta_z \gg \xi_{\perp}}^* \sim 5 \mu\text{s}$ corresponding to $\sigma_{\beta_z} \sim 40$ kHz. At the level anticrossing, the static strain ξ_{\perp} protects the central spin against first-order magnetic fluctuations leading to $T_{2,\beta_z=0}^* \sim 35 \mu\text{s}$, a value in the same range as the one obtained for single NV defects hosted in an isotopically purified diamond sample [Fig. 2(c)]. Here, decoherence is fixed by the intrinsic electric field noise $\sigma_{\xi_{\perp}}$ and second-order magnetic field fluctuations ($\sigma_{\beta_z}^2/2\xi_{\perp} \sim 5$ kHz), which are reaching the same order of magnitude. In this regime, the simple model leading to Eq. (3) is not valid and it is not possible to extract a simple analytic formula describing the full evolution of T_2^* around the anticrossing [26].

We note that the linewidth of the coherence peak reaches $\Delta B_z \sim 10$ mG ($\Delta\beta_z \sim 30$ kHz). Such a narrow linewidth can be exploited to detect individual ^{13}C nuclear spins weakly interacting with the NV defect through hyperfine coupling.

This interaction can be modeled as an effective magnetic field, leading to a Zeeman shift of the ESR frequencies $\beta_h = \mathcal{A}_C m_I$, where \mathcal{A}_C is the hyperfine coupling strength, which depends on the lattice site occupied by the ^{13}C impurity [34,35], and $m_I = \pm 1/2$ is the nuclear spin projection along the NV axis. Level anticrossings are then reached when $\beta_z + \beta_h = 0$, i.e., for $\beta_z = \pm \mathcal{A}_C/2$. Two coherence peaks can thus be observed around zero field, whose splitting is fixed by the hyperfine coupling strength (Fig. 3). This method enables one to detect weakly coupled ^{13}C nuclei, e.g., $\mathcal{A}_C \sim 50$ kHz in Fig. 3(b).

We now analyze how T_2^* evolves around level anticrossings while modifying the electric noise $\sigma_{\xi_{\perp}}$ surrounding the NV defect. To this end, we first investigate NV defects artificially created close to the surface of a high-purity diamond crystal ($[^{13}\text{C}] = 1.1\%$) through the implantation of ^{15}N ions at 10 keV. The diamond sample was then annealed for 2 h in vacuum at 800°C , and its surface cleaned with acids. The resulting NV defects are located at roughly 15 nm below the diamond surface and are associated with the ^{15}N isotope, which is an $I = 1/2$ nucleus characterized by a hyperfine coupling strength $\mathcal{A}_{^{15}\text{N}} = 3.15$ MHz [36]. A typical evolution of T_2^* as a function of B_z for a near-surface NV defect is shown in Fig. 4(a). Two coherence peaks are observed at $\beta_z = \pm \mathcal{A}_{^{15}\text{N}}/2$, with a much smaller amplitude than the one observed for native NV defects placed a few micrometers below the surface [Figs. 2(c) and 3]. For shallow-implanted defects, the electric field noise contribution $\sigma_{\xi_{\perp}}$ is expected to increase significantly, owing to the close vicinity of fluctuating charges lying on the diamond surface [37]. Magnetic field fluctuations, which are also increased for near-surface NV defects [38], remain however the strongest source of noise, resulting in an

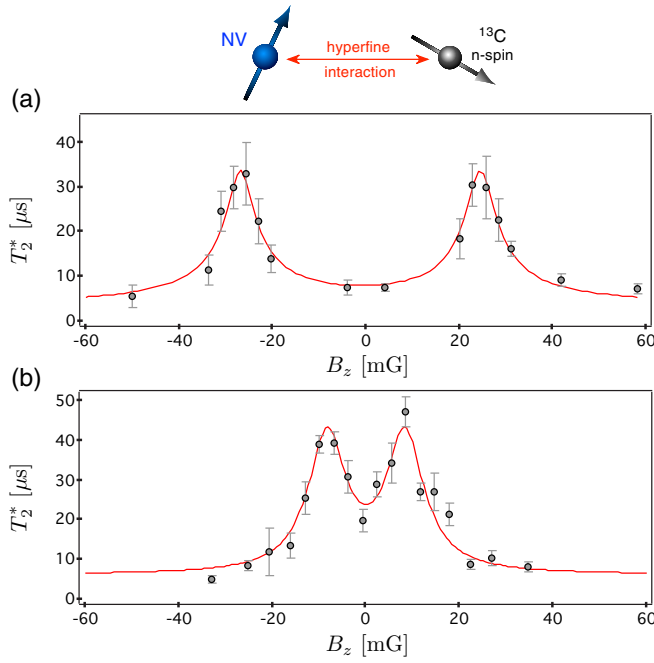


FIG. 3. T_2^* as a function of B_z for two different single NV defects coupled with a nearby ^{13}C nuclear spin. The solid lines are data fitting with two Lorentzian functions. The hyperfine coupling strength extracted from the fit are (a) $\mathcal{A}_C = 144 \pm 2$ kHz and (b) $\mathcal{A}_C = 47 \pm 2$ kHz.

enhanced coherence time at the level crossings ($\mathcal{R} > 1$). For NV defects implanted closer to the surface (~ 5 nm) of an isotopically purified diamond sample, it was recently shown that decoherence could be dominated by electric field noise, even far away from the level anticrossings [37]. In this case, the longitudinal component of the Stark effect $\xi_{\parallel} = d_{\parallel}\Pi_z/h$ needs to be included in the model. Assuming that decoherence is dominated by electric field noise—regardless of the applied magnetic field—the parameter \mathcal{R} defined by Eq. (4) becomes $\mathcal{R} = \sigma_{\xi_{\parallel}}/\sigma_{\xi_{\perp}} = d_{\parallel}/d_{\perp}$, where $\sigma_{\xi_{\parallel}}$ is the variance of the electric field fluctuations along the z axis [26]. In this case, a huge *dip* of T_2^* should therefore be observed around the level anticrossing ($\mathcal{R} \approx 1/50$). We note that in Ref. [37], the coherence time was inferred through dynamical decoupling sequences which are not sensitive to the same frequencies of the noise spectrum as Ramsey spectroscopy. Combining both approaches around level anticrossings might be used in the future to infer the spectral density of the electric field noise surrounding near-surface NV defects.

In an attempt to access a regime with a larger contribution of the electric noise, we finally investigate single NV defects hosted in commercially available nanodiamonds (NDs) produced by milling type-Ib high-pressure high-temperature (HPHT) diamond crystals. The formation of NV defects was carried out using high-energy (13.6 MeV) electron irradiation followed by annealing at 800°C under vacuum. The irradiated NDs were then oxidized in air at 550°C for 2 h in order to remove graphitic-related defects on the surface and produce stable NV defects [39]. The evolution of T_2^* as a function of B_z for a single NV defect hosted in a 30-nm ND is shown in Fig. 4(b). A pronounced *dip* of the coherence time is observed at the level anticrossing, which indicates that $\sigma_{\xi_{\perp}} > \sigma_{\beta_z}$ in this ND. This

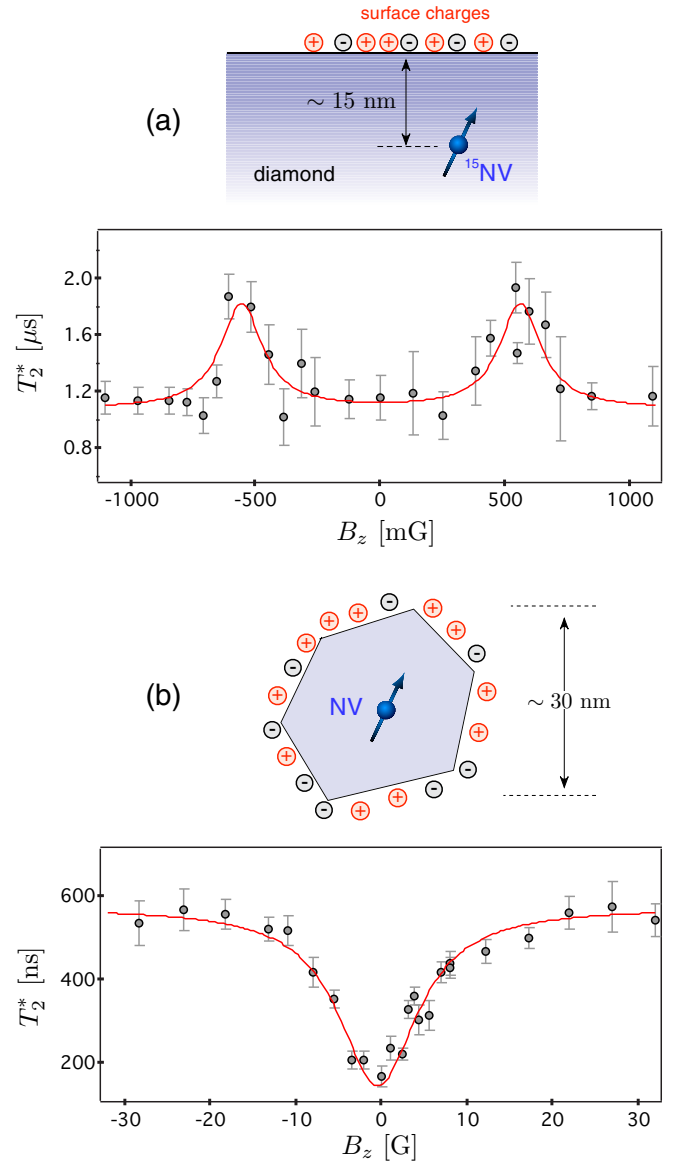


FIG. 4. (a) T_2^* as a function of B_z for a single NV defect implanted at ~ 15 nm below the surface of a high-purity diamond sample ($[^{13}\text{C}] = 1.1\%$). The static strain is $\xi_{\perp} = 230$ kHz. (b) Same experiment realized for a single NV defect hosted in a 30-nm ND. The solid line is data fitting with Eq. (3). Here, the static strain is $\xi_{\perp} = 7$ MHz.

situation is similar to the one observed for native NV defects hosted in isotopically purified diamond samples [Fig. 2(c)]. Data fitting with Eq. (3) leads to $\sigma_{\beta_z} = 409 \pm 7$ kHz and $\sigma_{\xi_{\perp}} = 1360 \pm 50$ kHz. We note that the width of the *dip* is much larger than the one observed in bulk diamond samples, because the static strain reaches a few MHz for NV defects hosted in NDs.

Using Ramsey spectroscopy around a level anticrossing, we have analyzed the competition between electric field and magnetic field fluctuations in the decoherence of the electronic spin associated with single NV defects in different types of diamond samples. To this end, we have used a static magnetic field to switch the spin system between eigenstates protected either against magnetic noise or against electric noise. This study provides significant insights into the decoherence of

the NV electronic spin, thus giving different perspectives of performance optimization in quantum metrology and sensing applications [15–17].

ACKNOWLEDGMENTS

We thank R. B. Liu and P. Maletinsky for fruitful discussions and careful reading of the manuscript. This

research has been supported by the European Union Seventh Framework Program (FP7/2007-2013) under the project DIADEMS and by the European Research Council under the grants ERC-StG-2014, IMAGINE and ERC-CoG-2013, CIRQUSS (Grant Agreement No. 615767). J.R.M acknowledges support from Conicyt-PIA Grants No. ACT1108 and No. ACT1112, Fondecyt Grant No. 1141185, and Air Force FA9550-15-1-0113.

-
- [1] G. Balasubramanian, P. Neumann, D. Twitchen, M. Markham, R. Kolesov, N. Mizusochi, J. Isoya, J. Achard, J. Beck, J. Tisler, V. Jacques, P. R. Hemmer, F. Jelezko, and J. Wrachtrup, *Nat. Mater.* **8**, 383 (2009).
- [2] N. Mizuochi, P. Neumann, F. Rempp, J. Beck, V. Jacques, P. Siyushev, K. Nakamura, D. J. Twitchen, H. Watanabe, S. Yamasaki, F. Jelezko, and J. Wrachtrup, *Phys. Rev. B* **80**, 041201(R) (2009).
- [3] A. M. Tyryshkin, S. Tojo, J. J. L. Morton, H. Riemann, N. V. Abrosimov, P. Becker, H.-J. Pohl, T. Schenkel, M. L. W. Thewalt, K. M. Itoh, and S. A. Lyon, *Nat. Mater.* **11**, 143 (2012).
- [4] D. Stepanenko, G. Burkard, G. Giedke, and A. Imamoglu, *Phys. Rev. Lett.* **96**, 136401 (2006).
- [5] H. Bluhm, S. Foletti, D. Mahalu, V. Umansky, and A. Yacoby, *Phys. Rev. Lett.* **105**, 216803 (2010).
- [6] E. Togan, Y. Chu, A. Imamoglu, and M. D. Lukin, *Nature (London)* **478**, 497 (2011).
- [7] A. Dréau, P. Jamonneau, O. Gazzano, S. Kosen, J.-F. Roch, J. R. Maze, and V. Jacques, *Phys. Rev. Lett.* **113**, 137601 (2014).
- [8] L. Viola, E. Knill, and S. Lloyd, *Phys. Rev. Lett.* **82**, 2417 (1999).
- [9] J. Du, X. Rong, N. Zhao, Y. Wang, J. Yang, and R. B. Liu, *Nature (London)* **461**, 1265 (2009).
- [10] G. de Lange, Z. H. Wang, D. Riste, V. V. Dobrovitski, and R. Hanson, *Science* **330**, 60 (2010).
- [11] X. Xu, Z. Wang, C. Duan, P. Huang, P. Wang, Y. Wang, N. Xu, X. Kong, F. Shi, X. Rong, and J. Du, *Phys. Rev. Lett.* **109**, 070502 (2012).
- [12] D. A. Golter, T. K. Baldwin, and H. Wang, *Phys. Rev. Lett.* **113**, 237601 (2014).
- [13] A. Barfuss, J. Teissier, E. Neu, A. Nunnenkamp, and P. Maletinsky, *Nat. Phys.* **11**, 820 (2015).
- [14] E. R. MacQuarrie, T. A. Gosavi, S. A. Bhave, and G. D. Fuchs, *Phys. Rev. B* **92**, 224419 (2015).
- [15] J. S. Hodges, N. Y. Yao, D. Maclaurin, C. Rastogi, M. D. Lukin, and D. Englund, *Phys. Rev. A* **87**, 032118 (2013).
- [16] L. Rondin, J.-P. Tetienne, T. Hingant, J.-F. Roch, P. Maletinsky, and V. Jacques, *Rep. Prog. Phys.* **77**, 056503 (2014).
- [17] R. Schirhagl, K. Chang, M. Loretz, and C. L. Degen, *Annu. Rev. Phys. Chem.* **65**, 83 (2014).
- [18] L. Childress and R. Hanson, *MRS Bull.* **38**, 134 (2013).
- [19] X. Zhu, S. Saito, A. Kemp, K. Kakuyanagi, S. Karimoto, H. Nakano, W. J. Munro, Y. Tokura, M. S. Everitt, K. Nemoto, M. Kasu, N. Mizuochi, and K. Semba, *Nature (London)* **478**, 221 (2011).
- [20] Y. Kubo, C. Grezes, A. Dewes, T. Umeda, J. Isoya, H. Sumiya, N. Morishita, H. Abe, S. Onoda, T. Ohshima, V. Jacques, A. Dréau, J.-F. Roch, I. Diniz, A. Auffeves, D. Vion, D. Esteve, and P. Bertet, *Phys. Rev. Lett.* **107**, 220501 (2011).
- [21] O. Arcizet, V. Jacques, A. Siria, P. Poncharal, P. Vincent, and S. Seidelin, *Nat. Phys.* **7**, 879 (2011).
- [22] F. Dolde, H. Fedder, M. W. Doherty, T. Nöbauer, F. Rempp, G. Balasubramanian, T. Wolf, F. Reinhard, L. C. L. Hollenberg, F. Jelezko, and J. Wrachtrup, *Nat. Phys.* **7**, 459 (2011).
- [23] M. W. Doherty, F. Dolde, H. Fedder, F. Jelezko, J. Wrachtrup, N. B. Manson, and L. C. L. Hollenberg, *Phys. Rev. B* **85**, 205203 (2012).
- [24] Ph. Tamarat, T. Gaebel, J. R. Rabeau, M. Khan, A. D. Greentree, H. Wilson, L. C. L. Hollenberg, S. Prawer, P. Hemmer, F. Jelezko, and J. Wrachtrup, *Phys. Rev. Lett.* **97**, 083002 (2006).
- [25] E. van Oort and M. Glasbeek, *Chem. Phys. Lett.* **168**, 529 (1990).
- [26] See Supplemental Material at <http://link.aps.org/supplemental/10.1103/PhysRevB.93.024305> for details concerning the experimental setup and the theoretical model used to describe decoherence of the NV defect as a function of electric and magnetic noise.
- [27] P. Neumann, R. Kolesov, V. Jacques, J. Beck, J. Tisler, A. Batalov, L. Rogers, N. B. Manson, G. Balasubramanian, F. Jelezko, and J. Wrachtrup, *New J. Phys.* **11**, 013017 (2009).
- [28] T. Teraji, *J. Appl. Phys.* **118**, 115304 (2015).
- [29] J. R. Maze, A. Dréau, V. Waselowski, H. Duarte, J.-F. Roch, and V. Jacques, *New J. Phys.* **14**, 103041 (2012).
- [30] K. Beha, A. Batalov, N. B. Manson, R. Bratschitsch, and A. Leitenstorfer, *Phys. Rev. Lett.* **109**, 097404 (2012).
- [31] N. Aslam, G. Waldherr, P. Neumann, F. Jelezko, and J. Wrachtrup, *New J. Phys.* **15**, 013064 (2013).
- [32] P. Siyushev, H. Pinto, M. Voros, A. Gali, F. Jelezko, and J. Wrachtrup, *Phys. Rev. Lett.* **110**, 167402 (2013).
- [33] E. Bourgeois, A. Jarmola, M. Gulka, J. Hruby, D. Budker, and M. Nesladek, [arXiv:1502.07551](https://arxiv.org/abs/1502.07551).
- [34] B. Smeltzer, L. Childress, and A. Gali, *New J. Phys.* **13**, 025021 (2011).
- [35] A. Dréau, J.-R. Maze, M. Lesik, J.-F. Roch, and V. Jacques, *Phys. Rev. B* **85**, 134107 (2012).
- [36] J. R. Rabeau, P. Reichart, G. Tamanyan, D. N. Jamieson, S. Prawer, F. Jelezko, T. Gaebel, I. Popa, M. Domhan, and J. Wrachtrup, *Appl. Phys. Lett.* **88**, 023113 (2006).
- [37] M. Kim, H. J. Mamin, M. H. Sherwood, K. Ohno, D. D. Awschalom, and D. Rugar, *Phys. Rev. Lett.* **115**, 087602 (2015).
- [38] B. K. Ofori-Okai, S. Pezzagna, K. Chang, M. Loretz, R. Schirhagl, Y. Tao, B. A. Moores, K. Groot-Berning, J. Meijer, and C. L. Degen, *Phys. Rev. B* **86**, 081406(R) (2012).
- [39] L. Rondin, G. Dantelle, A. Slablab, F. Grosshans, F. Treussart, P. Bergonzo, S. Perruchas, T. Gacoin, M. Chaigneau, H.-C. Chang, V. Jacques, and J.-F. Roch, *Phys. Rev. B* **82**, 115449 (2010).